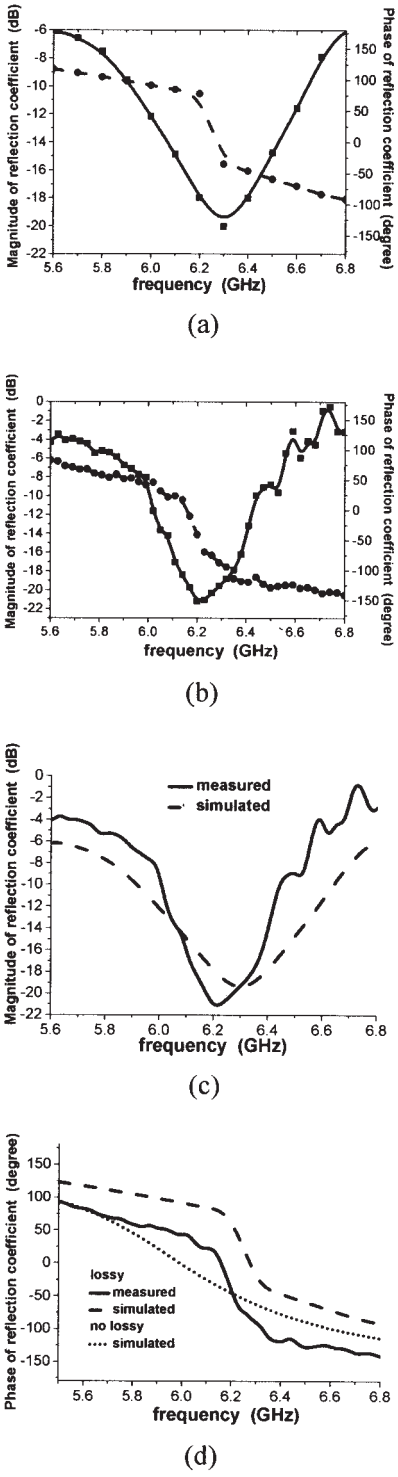


**Figure 4** Reflection coefficient of the ultra-thin absorber: (a) simulated reflection coefficient; (b) measured reflection coefficient; (c) comparison of magnitude; (d) comparison of phase

Figure 3 shows the function plot of Eq. (4). It is shown that $R_p$ reaches the minimum at $\phi = 0$, and the absorption deteriorates rapidly when $\phi$ increases.

However, $\phi$ is a nonlinear function of the frequency of the incident wave, and the region between $-\pi/2$ and $\pi/2$ corresponds to the forbidden frequency band of the HIGP. Thus, a broad absorption band can be expected if a proper HIGP with a broad forbidden frequency band is designed.

### *3.2. Numerical and Experimental Examples*

In this section, we consider the HIGP with the following parameters: $P = 7.2$ mm, $w = 6.8$ mm, $r = 0.4$ mm, $g = 1$ mm, $h = 1.5$ mm, and $\varepsilon = 2.65$. The lumped resistance $R = 375\Omega$. The absorption property of the ultra-thin absorber using the HIGP is shown in Figure 4.

It is seen that the electromagnetic wave is absorbed in the region 6.0–6.6 GHz, corresponding the absorption bandwidth of about 600 MHz. The absorption reaches maximum at $f_0 = 6.3$ GHz, which corresponds to the wavelength $\lambda_0 = 4.72$ cm. Since the lossy screen is very thin, the depth of the absorber is about that of the HIGP, that is, much less than the wavelength $h/\lambda_0 \approx 0.031$. The measured results basically agree well with the simulated ones, and from Figure 4(d) we can observe that the bandgap of the HIGP determines the bandwidth of the ultra-thin absorber.

## 5. CONCLUSION

In this paper, we have shown a novel RAM design using the Sievenpiper HIGP. The absorption performance of the RAM was determined by the high-impedance property of the HIGP; thus, we can obtain the expected absorption band by regulating the HIGP.

## REFERENCES

1. A.A. Zharov, I.V. Shadrivov, and Y.S. Kivshar, Nonlinear properties of left-handed metamaterials, PRL 91 (2003), 037401.
2. C. Caloz and T. Itoh, Positive/negative refractive index anisotropic 2D metamaterials, IEEE Microwave Wireless Compon Lett 13 (2003), 547–549.
3. D. Sievenpiper et al. High-impedance electromagnetic surface with a forbidden frequency band, IEEE Trans Microwave Theory Tech 47 (1999), 2059–2074.
4. L. Zhou and C.T. Chan, High-impedance reflectivity and surface-wave band gaps in metamaterials, APL (2004), 1444–1446.
5. F. Yang and Y. Rahmat-Samii, Reflection phase characterizations of the EBG ground plane for low-profile wire-antenna applications, IEEE Trans Antennas Propagat 51 (2003), 2691–2703.
6. N. Engheta, Thin absorbing screens using metamaterial surfaces, IEEE Antennas Propagat Soc (AP-S) Int Symp USNC/URSI Natl Radio Sci Mtg, San Antonio, TX, 2002, pp. 16–21.
7. D.J. Kern and D.H. Werner, A genetic algorithm approach to the design of ultra-thin electromagnetic bandgap absorbers, Microwave Opt Technol Lett 38 (2003), 61–64.
8. W.W. Salisbury, Absorbent body for electromagnetic waves, U.S. Patent 2 599 944, 1952.
9. R.L. Fante and M.T. McCormack, Reflection properties of the Salisbury screen, IEEE Trans Antennas Propagat 36 (1988), 1443–1454.
10. K.J. Vinoy and R.M. Jha, Radar-absorbing materials: From theory to design and characterization, Kluwer Academic Publishers, Boston, 1996.



# AN OPTIMUM ULTRA-WIDEBAND MICROSTRIP FILTER

**Jia-Sheng Hong and Hussein Shaman**
Department of Electrical, Electronic & Computer Engineering
Heriot-Watt University
Edinburgh, EH14 4AS, United Kingdom

*Received 7 May 2005*

**ABSTRACT:** *An ultra-wideband (UWB) microstrip filter with a fractional bandwidth (FBW) of more than 100% is designed and demonstrated. This UWB microstrip-filter design is based on a circuit model for an optimum short-circuited stub transmission-line filter whose unit*

*elements or connecting lines are nonredundant. A comparison study is carried out to show the advantages of this type of filter versus the conventional design, whose unit elements are redundant. The theoretical, simulated, and experimental results of the designed optimum UWB microstrip filter are presented.* © 2005 Wiley Periodicals, Inc. Microwave Opt Technol Lett 47: 230–233, 2005; Published online in Wiley InterScience (www.interscience.wiley.com). DOI 10.1002/mop.21133

**Key words:** *microstrip filters; ultra wideband (UWB) filters; transmission-line filters*

## 1. INTRODUCTION

Ultra-wideband (UWB) technology is being reinvented recently with many promising modern applications [1]. The rapid growth in this field has stimulated the development of wideband microwave filters [2–6]. Microstrip parallel coupled-line and interdigital-line filters are commonly known to be low-cost wideband bandpass filters, but very tight coupling gaps and high fabrication tolerances are required when the fractional bandwidth (FBW) becomes very large, for instance, larger than 50%. To lighten the requirement on very small coupling gaps of the conventional microstrip parallel coupled-line filter, a five-pole parallel-coupled three-line microstrip filter with a fractional bandwidth of 50% was demonstrated in [2]. Alternatively, an aperture-compensation technique was proposed for the effective enhancement of coupling strength in parallel-coupled microstrip line and a filter of this type exhibited FBW of 70% [3]. Microstrip-ring resonators loaded with short-circuited stubs have also been proposed for designing ultra-wideband filters with FBW of more than 100% [4]. The operation of the ring filter can be understood in such way that two stub-loaded transmission-line filters are connected in parallel. Another type of ring filter with loaded open stubs used to control attenuation poles has been introduced [5] and an UWB bandpass filter of this type with a passband from 3.8 to 9.2 GHz (FBW = 83%) has been experimentally demonstrated. More recently, a double-sided parallel-strip bandpass filter for a bandwidth from 4 to 6.5 GHz has been designed based on a short-circuited stub filter model [6].

In view of the aforementioned development of wideband planar filters, it is evident that the distributed stub transmission-line filter, although it may be modified and realized in different form such as the ring or double-sided parallel strip, appears more attractive for designing multipole or high-order selective UWB filters. The reason for this is twofold: (i) the tolerance for ultra-wideband multipole-coupled resonator filters is too high for low-loss fabrication, particularly when a high-order filter is required for high selectivity; (ii) it is difficult to realize lumped elements for UWB filters which operate over a very wide frequency bandwidth in gigahertz. To this end, this paper describes the design of UWB microstrip filters based on a circuit model for an optimum short-circuited stub filter whose unit elements or connecting lines are nonredundant. A comparison study is carried out to show the advantages of this type of filter versus the conventional design whose unit elements are redundant. The theoretical, simulated, and experimental results of the designed optimum UWB microstrip filter with a fractional bandwidth of more than 120% are presented.

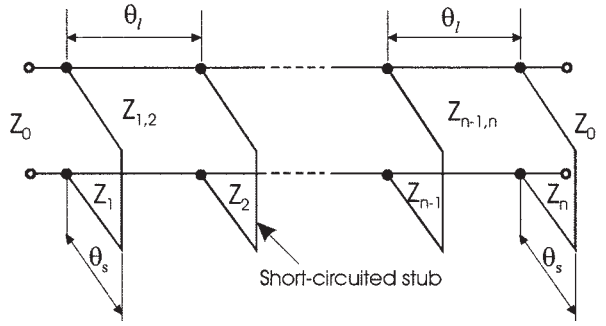


**Figure 1** Equivalent circuit of short-circuited stub filter

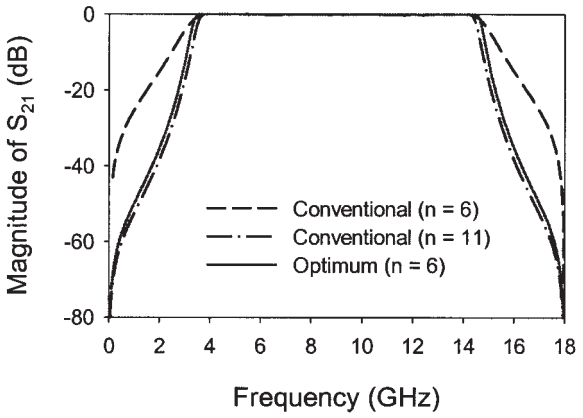


**Figure 2** Transmission characteristics of three UWB short-circuited stub filters with the same passband from 3.5 to 14.5 GHz

## 2. A GENERAL CIRCUIT MODEL

A general circuit model for a short-circuited stub filter is shown in Figure 1 and is comprised of a cascaded of $n$ shunt short-circuited stubs of electrical length $\theta_s$, separated by connecting transmission lines (unit elements) of electrical length $\theta_l$. Both $\theta_s$ and $\theta_l$ are determined at some characteristic frequency $f_c$, $Z_0$ is the terminal impedance. $Z_1, Z_2, \ldots Z_n$ are the line characteristic impedances of the short-circuited stubs. The characteristic impedances of the connecting lines are denoted by $Z_{1,2}$ to $Z_{n-1,n}$.

For our purposes, we have investigated different stub-filter designs for an UWB filter with a passband from 3.5 to 14.5 GHz, corresponding to a factional bandwidth of about 122% at a midband frequency 9 GHz. Figure 2 shows the frequency responses of three short-circuited stub filters for the comparison. For the two conventional stub filters, $\theta_s = \theta_l = 90°$ at $f_c = 9$ GHz, which is also the midband frequency; thus, all the short-circuited stubs and connecting lines are quarter wavelength long at the midband frequency. It is obvious that the conventional stub filter with 11 stubs ($n = 11$) has a higher selectivity than the conventional stub filter with six stubs ($n = 6$). Nevertheless, this indicates that a larger number of short-circuited stubs are usually necessary for this type of UWB filter requiring high selectivity. The design of conventional stub filters is well documented in [7]. For our subsequent discussion, Table 1 lists the designed circuit parameters of the conventional stub filter with 11 short-circuited stubs.

**TABLE 1 Circuit Parameters for a Conventional Short-Circuited Stub Filter with 11 Stubs for an Ultra-Wide Passband from 3.5 to 14.5 GHz ($\theta_s = \theta_l = 90°$ at 9 GHz)**

| Stub-Line Impedance | Connecting-Line Impedance |
|---|---|
| $Z_1 = Z_{11} = 199.07\Omega$ | $Z_{1,2} = Z_{10,11} = 38.84\Omega$ |
| $Z_2 = Z_{10} = 101.88\Omega$ | $Z_{2,3} = Z_{9,10} = 36.73\Omega$ |
| $Z_3 = Z_9 = 101.76\Omega$ | $Z_{3,4} = Z_{8,9} = 38.95\Omega$ |
| $Z_4 = Z_8 = 98.49\Omega$ | $Z_{4,5} = Z_{7,8} = 39.73\Omega$ |
| $Z_5 = Z_7 = 97.41\Omega$ | $Z_{5,6} = Z_{6,7} = 40.00\Omega$ |
| $Z_6 = 97.13\Omega$ | — |

**TABLE 2 Circuit Parameters for an Optimum Short-Circuited Stub Filter with Six Stubs for an Ultra-Wide Passband from 3.5 to 14.5 GHz ($\theta_s = 35°$ and $\theta_l = 70°$ at 3.5 GHz)**

| Stub-Line Impedance | Connecting-Line Impedance |
|---|---|
| $Z_1 = Z_6 = 103.96\Omega$ | $Z_{1,2} = Z_{5,6} = 48.85\Omega$ |
| $Z_2 = Z_5 = 72.64\Omega$ | $Z_{2,3} = Z_{4,5} = 50.44\Omega$ |
| $Z_3 = Z_4 = 64.48\Omega$ | $Z_{3,4} = 50.82\Omega$ |

The third filter whose frequency response is also shown in Figure 2 is an optimum stub filter, which has also only six stubs ($n = 6$). For this optimum stub filter, the electrical length of the short-circuited stubs is $\theta_s = 35°$ while the electrical length of the connecting lines or unit elements is $\theta_l = 2\theta_s = 70°$ at $f_c = 3.5$ GHz. From Figure 2, it can be noted that the optimum stub filter with six short-circuited stubs achieves the same selectivity as the conventional stub filter that requires eleven short-circuited stubs. This is because the unit elements of the optimum stub filter are not redundant, and they function nearly as effectively as the short-circuited stubs in improving the selectivity.

To determine the circuit parameters of an optimum stub filter, in practice, a computer-aided synthesis program is required. As an alternative, tabulated elements can be found in [8] for this type of filter, which is also seen as the optimum pseudo-highpass filter. For the optimum stub filter discussed above, the circuit parameters are given in Table 2. Comparing the circuit parameters in Tables 1 and 2, we can see that in order to have the same filtering characteristics shown in Figure 2, the first and last stubs of the conventional filter need an extremely high characteristic impedance of 199.07Ω. Such a high impedance level will result in a very narrow line, which can be very difficult to realize in microstrip using a low-cost fabrication technology. On the other hand, the optimum stub filter has much more reasonable impedance levels for all the short-circuited stubs. Moreover, the characteristic impedances of the connecting lines are all close to the terminal impedance of 50Ω. As a matter of fact, with a slight modification, all the connecting lines can be made to have a 50Ω characteristic impedance. Since the unit elements of the optimum stub filter also account for the order or degree of the filter, another advantage of the optimum stub filter is that it has the fewest number of T-junctions for the same order (11 in this case) of the conventional stub filter. In addition, the separations between adjacent stubs are wider for $\theta_l = 70°$ at 3.5 GHz, resulting in the least interactions between neighboring stubs or junctions.

## 3. SIMULATION AND EXPERIMENT

Based on circuit parameters given in Table 2, an optimum UWB microstrip filter has been designed on a 1.27-mm-thick RT/Duroid 6006 substrate with a relative dielectric constant of 6.15. The layout of the designed microstrip filter is shown in Figure 3. All the connecting lines or unit elements have been modified to have a characteristic impedance of 50Ω, so the filter has a very simple structure of a straight 50Ω line loaded with six short-circuited stubs. The narrowest stub line has a width of 0.3 mm, which can

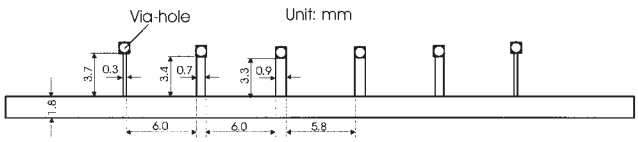


**Figure 3** Optimum UWB microstrip filter on a dielectric substrate with relative dielectric constant of 6.15 and thickness of 1.27 mm

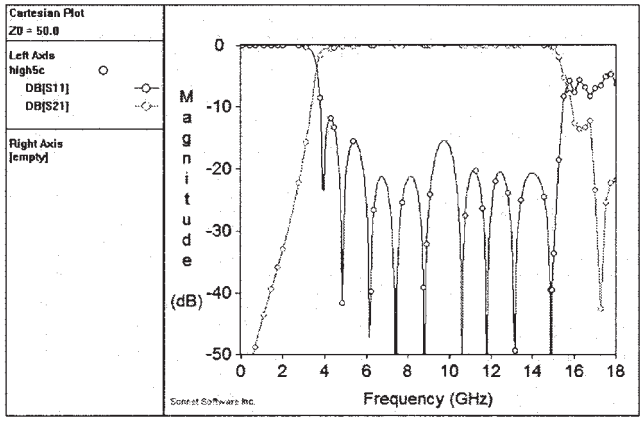


**Figure 4** EM-simulated performance of the optimum UWB microstrip filter in Fig. 3

be easily fabricated using a low-cost printed circuit-board (PCB) technology. The filter dimensions indicated on the layout have been taken into account the effects of T-junction discontinuities. Also, when determining the electrical length, a nominal characteristic frequency $f_c = 4$ GHz has been used instead of 3.5 GHz because the substrate used tends to shift down the frequency response. The design of the optimum UWB microstrip filter was verified firstly by full-wave EM simulation. The simulated results obtained using commercially available software [9] are plotted in Figure 4. In the simulation, the filter was enclosed in a metallic box and the minimum cell size used was 50 $\mu$m. Even though there were some box modes occurring at high frequencies (around 16 GHz), as well as numerical tolerances due to the finite cell sizes, in general, the EM simulation exhibited the desired frequency responses for the designed filter.

For the experimental demonstration, the designed filter was fabricated using a conventional PCB technology, as illustrated by a photograph of the fabricated filter in Figure 5. The size of the filter is quite compact, occupying an effective circuit area of 34 × 6 mm only. For the measurement, the input and output ports were extended to connect to two SMA connectors. The via-hole grounds were implemented simply via soldering. The fabricated filter was measured using an HP network analyzer, and the measured results without any tuning or trimming are plotted in Figure 6. We can see that although the filter has only six stubs along a 50Ω line, its measured $S_{11}$ frequency response does show 11 ripples in the passband, similar to a typical 11-pole Chebyshev filter characteristic. The measured bandwidth was 10.65 GHz at a midband frequency of 8.9 GHz, equivalent to a factional bandwidth of about 120%, which is in good agreement with the design and the simulation. The insertion loss at the midband was measured to be 0.75

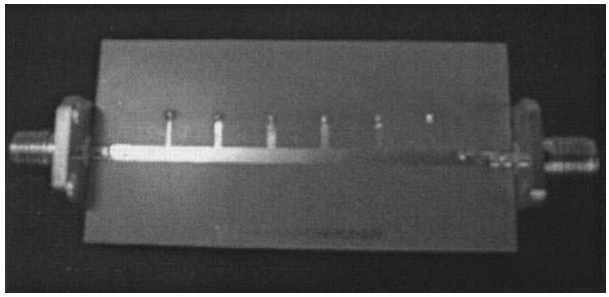

**Figure 5** Photograph of the fabricated optimum UWB microstrip filter

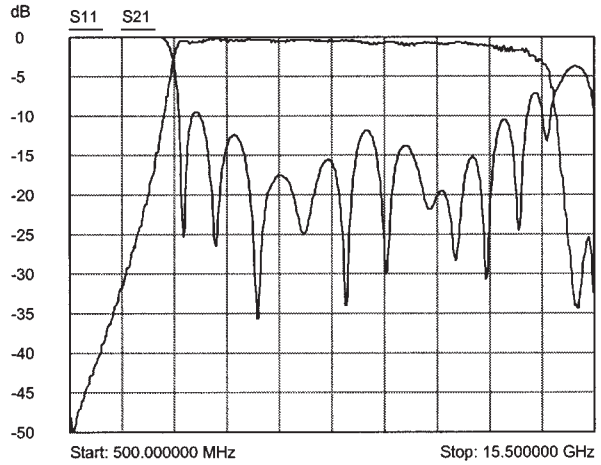


**Figure 6** Measured performance of the optimum UWB microstrip filter

dB. The insertion loss tended to increase towards higher frequencies, which would account for the frequency-dependent losses of the two SMA connectors and the dielectric material.

## 4. CONCLUSION

An ultra-wideband microstrip filter has been demonstrated. The filter has been designed based on a circuit model for an optimum short-circuited stub filter whose unit elements or connecting lines are nonredundant. It has been shown theoretically and experimentally that the connecting lines of the filter can function as effectively as the short-circuited stubs with regard to selectivity. The fabricated optimum UWB microstrip filter, equivalent to an 11-pole filter, has a very compact size. The measured bandwidth was 10.65 GHz at a midband frequency of 8.9 GHz for a factional bandwidth of about 120%. The measured midband insertion was 0.75 dB. The compact size, excellent wideband performance, and low-cost fabrication make this optimum stub filter a promising candidate for UWB applications.

## REFERENCES

1. Mini Special Issue on Ultra-Wideband, IEEE Trans Microwave Theory Tech 52 (2004).
2. J.-T. Kuo and E. Shih, Wideband bandpass filter design with three-line microstrip structures, IEEE MTT-S Int Microwave Symp Dig, Phoenix, AZ, (2001), 1593–1596.
3. L. Zhu, H. Bu, and K. Wu, Aperture compensation technique for innovative design of ultra-broadband microstrip bandpass filter, IEEE MTT-S Int Microwave Symp Dig, Boston, MA, (2000), 315–318.
4. H.-R. Ahn, I. Wolff, and N.-H. Myung, Small-sized wideband CVT- and CCT-ring filters, IEEE MTT-S Int Microwave Symp Dig, Philadelphia, PA, (2003), 1607–1610.
5. H. Ishida and K. Araki, Design and analysis of USB bandpass filter with ring filter, IEEE MTT-S Int Microwave Symp Dig (2004), 1307–1310.
6. S.-G. Kim and K. Chang, Ultrawide-band transitions and new microwave components using double-sided parallel-strip lines, IEEE Trans Microwave Theory Tech 52 (2004), 2148–2152.
7. G. Mattaei, L. Young, and E.M.T. Jones, Microwave filters, impedance-matching networks, and coupling structures, Artech House, Norwood, MA, 1980.
8. J.-S. Hong and M.J. Lancaster, Microstrip filters for RF/microwave applications, J Wiley, New York, 2001.
9. Sonnet Software Inc., EM user's manual, Ver. 9, 2003.



# A HIGH-EFFICIENCY INTERNAL WLAN ANTENNA FOR WIRELESS DEVICES OPERATING IN CLOSE PROXIMITY TO A LOSSY MEDIUM

**Kin-Lu Wong, Chih-Hua Chang, and Chun-I Lin**
Department of Electrical Engineering
National Sun Yat-Sen University
Kaohsiung 80424, Taiwan

*Received 4 May 2005*

**ABSTRACT:** *This paper presents a dual-loop patch antenna capable of providing high radiation efficiency for operation in close proximity to a lossy medium with permittivity and conductivity close to those of a human torso or arm. For operation as an internal WLAN (wireless local area network) antenna in a wireless device, the dual-loop patch antenna with a low profile of 3 mm can cover the operating bandwidth of the 2.4-GHz band (2400–2484 MHz), showing a high radiation efficiency of about 88%, when placed very close to the lossy medium with only 1-mm spacing. The obtained results make the proposed antenna very promising for body-worn or wearable antenna applications.* © 2005 Wiley Periodicals, Inc. Microwave Opt Technol Lett 47: 233–236, 2005; Published online in Wiley InterScience (www.interscience.wiley.com). DOI 10.1002/mop.21134

**Key words:** *antennas; patch antennas; antennas in close proximity to a lossy medium; WLAN antennas; body-worn antennas*

## 1. INTRODUCTION

Body-worn or wearable antennas are usually employed in the vicinity of a human torso or arm [1–4]. Due to the presence of the human body, which functions as a lossy medium, the radiation performances of conventional antennas are usually greatly degraded. Recently, a compact shorted patch antenna showing a radiation efficiency of about 60% when operated in close proximity to a lossy medium was demonstrated [5]. In this paper, we propose a novel dual-loop patch antenna capable of providing a much higher radiation efficiency (about 90%) for body-worn antenna applications. The proposed antenna also shows a thin profile and is thus suitable to be employed in a wireless-communication device as an internal antenna. For this kind of application, the proposed antenna functions as a balanced-type structure [6–8] and can lead to a much reduced and unbalanced current flow on the system ground plane of the wireless device. This in turn will lead to greatly reduced possible coupling between the proposed antenna and the human body, even when the wireless device is placed very close to the human body. In this case, very minor degrading effects on the radiation performances of the proposed antenna can be expected. The details of the proposed antenna for 2.4-GHz WLAN operation [9] are described in this paper. The characteristics of the proposed antenna in close proximity to a lossy medium of fluid with its permittivity and conductivity close to those of a human torso or arm are studied.

## 2. THE PROPOSED ANTENNA WITH A LOSSY MEDIUM

Figure 1(a) shows the configuration of the proposed dual-loop patch antenna operating in close proximity to a lossy medium of fluid of relative permittivity 76 and conductivity 2.0 S/m, which are close to those of a human torso or arm at 2.4 GHz [3]. Figure 1(b) shows the side view of the configuration studied, and the detailed dimensions of the dual-loop radiating patch are given in Figure 1(c). Note that the dual-loop radiating patch is mounted above a ground plane of dimensions $60 \times 100$ mm$^2$, which is